Physical properties of galaxies at high redshifts III

- Galaxy Morphology

Galaxy bimodality at low redshifts

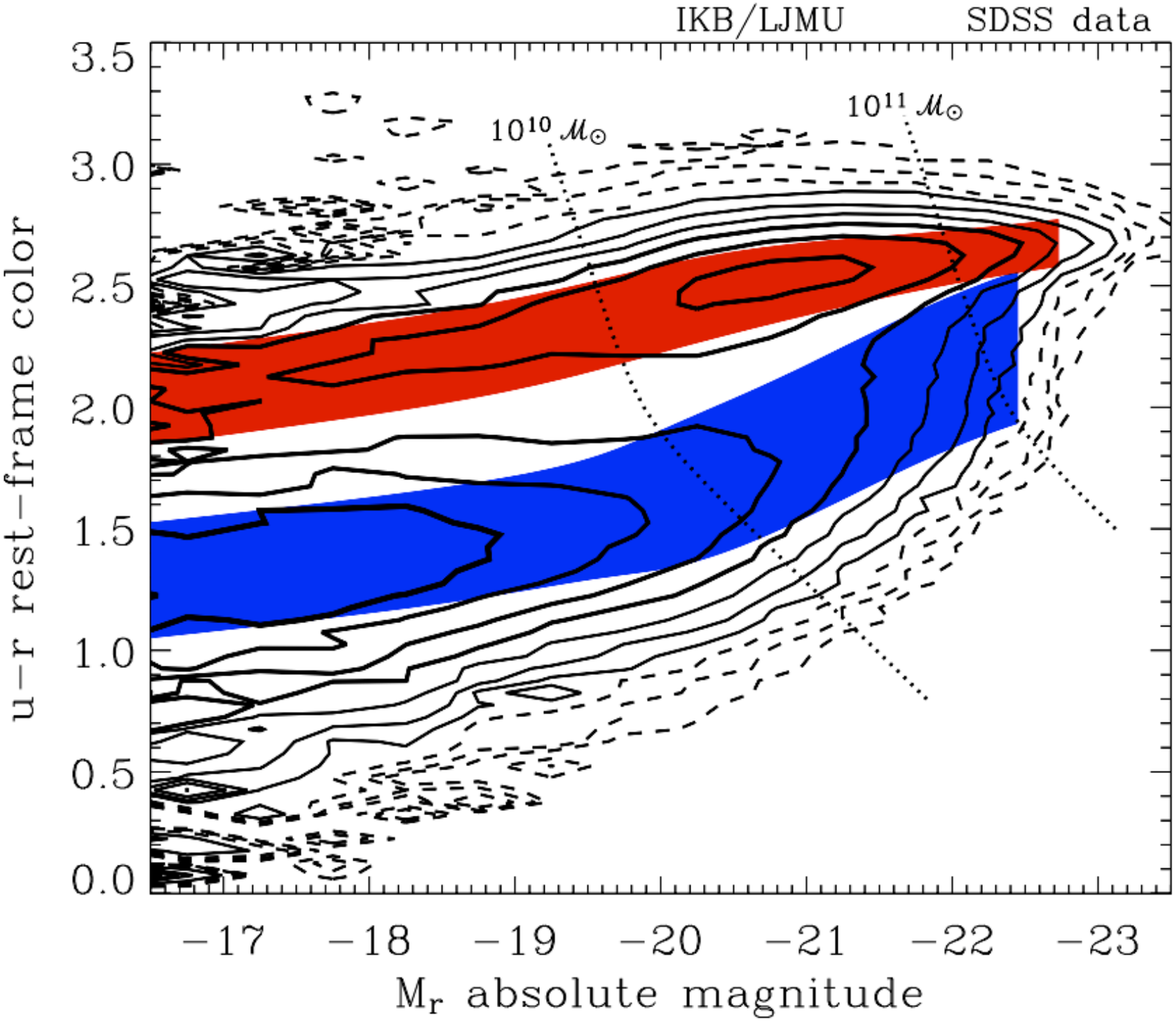

The red sequence is dominated by spheroids: ellipticals or S0 with large bulges

sample of galaxies from the Sloan Digital Sky Survey
(2400 deg2, 0:004 < z < 0:08, 23:5 < M r < 15:5)

Color functions for the galaxy distributions in absolute magnitude bins of width 0.5. Each plot shows galaxy number counts vs. rest-frame u-r color.

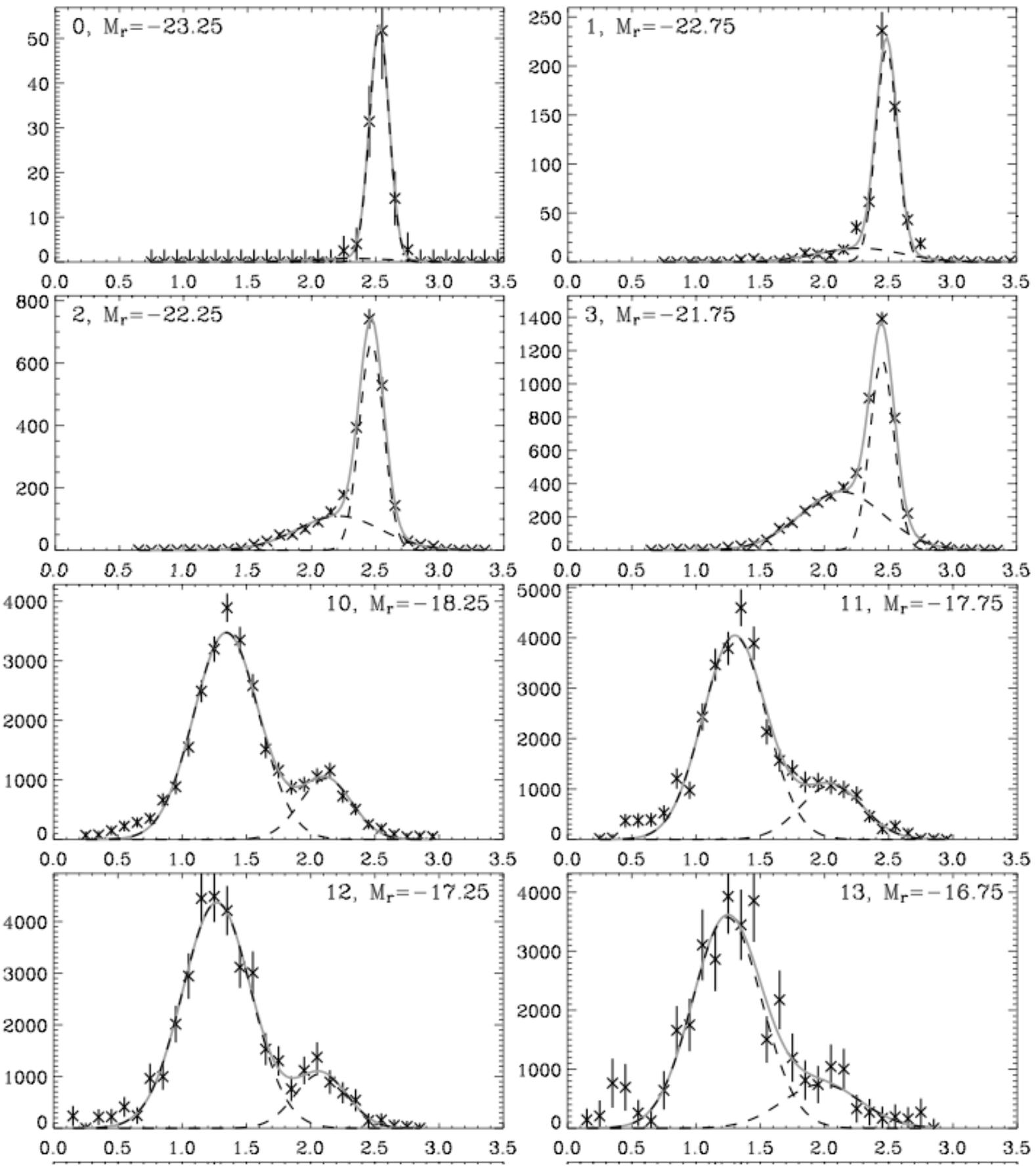

Baldry et al 2004

Color–mass relation at $1.8 < z < 2.2$. The $U - V$ color is corrected for reddening. Objects detected at 24μm are shown as filled gray circles. The hatched region indicates the approximate 90% completeness limit for red-sequence objects at $z = 2$.

The color bar in the right panel shows the median sSFR as a function of dust-corrected color

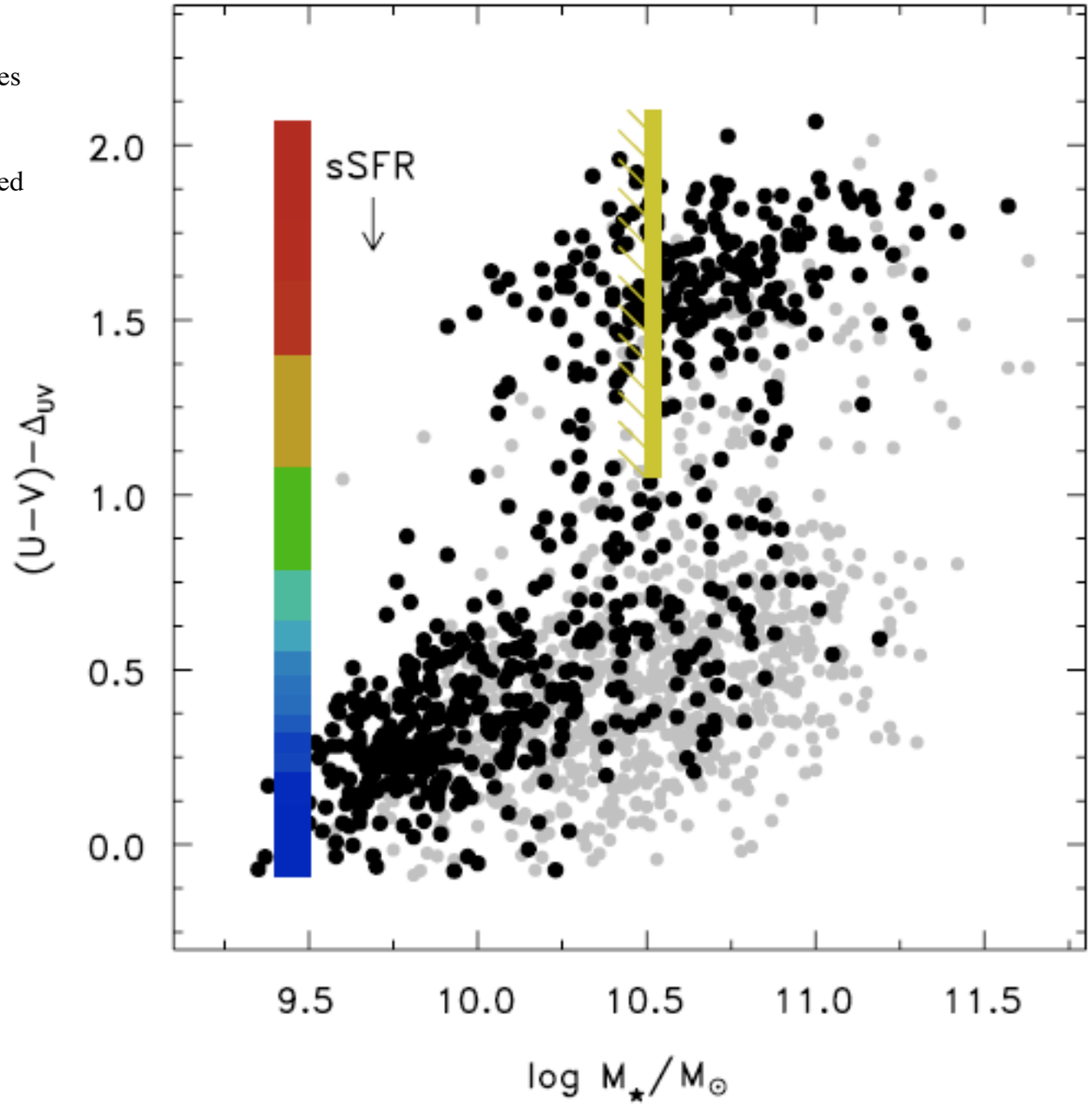

the cloud of galaxies with red dust corrected colors do, in fact, have very low sSFR.

The rest-frame U – V *c*olor distribution at all z=2.5 is bimodal, with a red peak, a blue peak, and a population of galaxies in between (the green valley).

We select 25,000 galaxies from the NEWFIRM Medium Band Survey (NMBS) to study the rest-frame $U - V$ color distribution of galaxies at $0 < z$ 2.5. The five unique NIR filters of the NMBS enable the precise measurement of photometric redshifts and rest-frame colors for 9900 galaxies at $1 < z < 2.5$.

Brammer et al ApJ 706:L173–L177, 2009

The Morphologies of Massive Galaxies at $1 < z < 3$ in the CANDELS-UDS Field: Compact Bulges, and the Rise and Fall of Massive Disks

Bruce etal. arXiv:1301.6373

In addition to the basic question of how high-redshift galaxies evolve in size, there is also still much debate about how these massive galaxies evolve in terms of their fundamental morphological type. Extensive studies of the local Universe have revealed a bimodality in the colour-morphology plane, with spheroidal galaxies typically inhabiting the red sequence and disk galaxies making up the blue cloud

At high z's a significant population of passive disk-dominated galaxies, providing evidence that the physical processes which quench star-formation may be distinct from those responsible for driving morphological transformations. This result is particularly interesting in light of the latest morphological studies of high-redshift massive galaxies by Buitrago et al. (2013) and van der Wel et al. (2011) who find that, in contrast to the local population of massive galaxies (which is dominated by bulge morphologies), ***by z ≃ 2 massive galaxies are predominantly disk-dominated systems***.

We use high-resolution, HSTWFC3/IR, near-infrared imaging to conduct a detailed bulge-disk decomposition of the morphologies of ≃200 of the most massive ($M_* > 10^{11} M_\odot$) galaxies at 1<z<3 in the CANDELS-UDS field.

For this study we have constructed a sample based on photometric redshifts and stellar mass estimates which were determined using the stellar population synthesis models of Bruzual & Charlot (2003) assuming a Chabrier initial mass function (see Bruce et al. 2012 for full details).

This provides us with a total mass-complete sample of ~ 200 galaxies.

We have employed the GALFIT (Peng et al. 2002) morphology fitting code to determine the morphological properties for all the objects in our sample.

To conduct the double component fitting we define three components: a S´ersic index fixed at n = 4 bulge, an n = 1 fixed disk and a centrally concentrated PSF component to account for any AGN or nuclear starbursts within our galaxies.

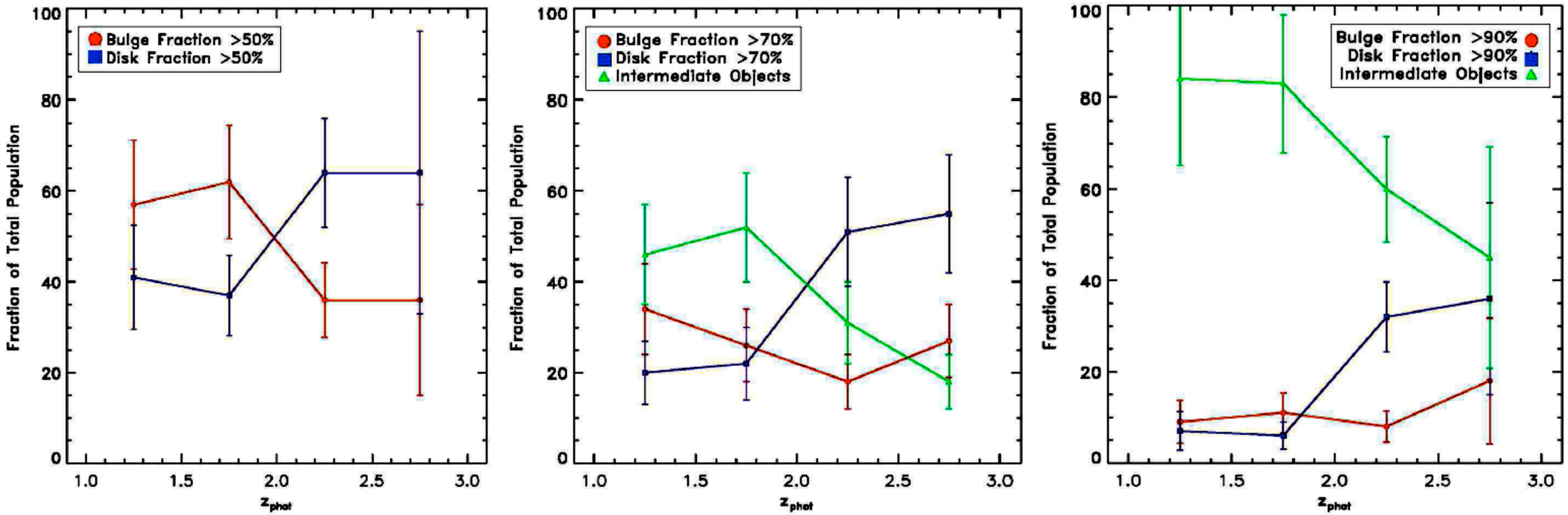

The redshift evolution of the morphological fractions in our galaxy sample, after binning into redshift bins of width z = 0.5 and using three alternative cuts in morphological classification

three alternative cuts in morphological classification as measured by B/T from bulge-disk decompositions.

In the left-hand panel of Fig. 1 we have simply split the sample into two categories: bulge-dominated ($B/T > 0.5$) and disk- dominated ($B/T < 0.5$).

In the central panel we have separated the sample into three categories, with any object for which $0.3 < B/T < 0.7$ classed as “Intermediate”.

In the right-hand panel we have expanded this Intermediate category to encompass all objects for which $0.1 < B/T < 0.9$.

$z \simeq 2$ marks a key transition phase, above which massive galaxies are predominantly disk-dominated systems and below which they become increasingly mixed bulge+disk systems.

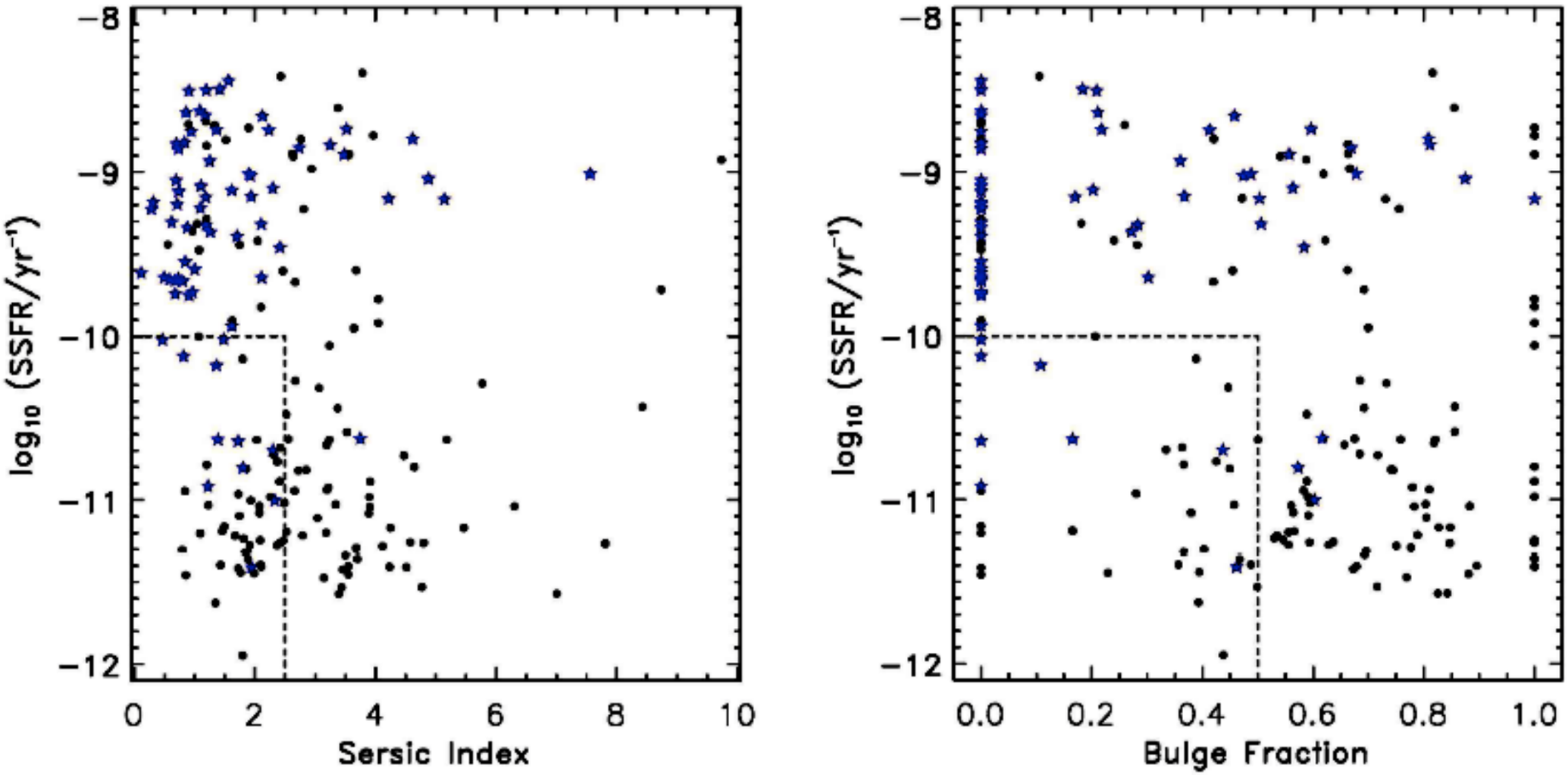

To first order, our results show that the well-documented bimodality in the colour-morphology plane seen at low redshift, where spheroidal galaxies inhabit the red sequence, while disk galaxies occupy the blue cloud is at least partly already in place by $z \simeq 2$.

Nonetheless, the sample also undoubtedly contains star-forming bulge-dominated galaxies and, perhaps more interestingly, a significant population of apparently quiescent disk-dominated objects.

The presence of a significant population of passive disks among the massive galaxy population at these redshifts indicates that star-formation activity can cease without a disk galaxy being turned directly into a disk-free spheroid, as generally previously expected if the process that quenches star formation is a major merger.

One possible mechanism for this arises from the latest generation of hydrodynamical simulations (e.g. Keres et al. 2005, Dekel et al. 2009a) and analytic theories (e.g. Birnboim & Dekel 2003), which suggest a formation scenario whereby at high redshift star-formation is fed through inflows of cold gas.

Another scenario which can account for star-formation quenching, whilst still being consistent with the existence of passive disks, is the model of violent disk instabilities (e.g. Dekel et al. 2009b), coupled with “morphology quenching” (Martig et al. 2009).

The morphologies of massive galaxies at $1 < z < 3$ in the CANDELS-UDS field: compact bulges, and the rise and fall of massive discs

We have used high-resolution, *Hubble Space Telescope*, near-infrared imaging to conduct a detailed analysis of the morphological properties of the most massive galaxies at high redshift, modelling the WFC3/IR H_{160}-band images of the $\simeq$200 galaxies in the CANDELS-UDS field with photometric redshifts $1 < z < 3$, and stellar masses $M_* > 10^{11}\,\mathrm{M}_\odot$. We have explored the results of fitting single-Sérsic and bulge+disc models, and have investigated the additional errors and potential biases introduced by uncertainties in the background and the on-image point spread function. This approach has enabled us to obtain formally acceptable model fits to the WFC3/IR images of >90 per cent of the galaxies. Our results indicate that these massive galaxies at $1 < z < 3$ lie both on and below the local size–mass relation, with a median effective radius of $\sim$2.6 kpc, a factor of $\simeq$2.3 smaller than comparably massive local galaxies. Moreover, we find that bulge-dominated objects in particular show evidence for a growing bimodality in the size–mass relation with increasing redshift, and by $z > 2$ the compact bulges display effective radii a factor of $\simeq$4 smaller than local ellipticals of comparable mass. These trends also appear to extend to the bulge components of disc-dominated galaxies. In addition, we find that, while such massive galaxies at low redshift are generally bulge-dominated, at redshifts $1 < z < 2$ they are predominantly mixed bulge+disc systems, and by $z > 2$ they are mostly disc-dominated. The majority of the disc-dominated galaxies are actively forming stars, although this is also true for many of the bulge-dominated systems. Interestingly, however, while most of the quiescent galaxies are bulge-dominated, we find that a significant fraction (25–40 per cent) of the most quiescent galaxies, with specific star formation rates $\mathrm{sSFR} < 10^{-10}\,\mathrm{yr}^{-1}$, have disc-dominated morphologies. Thus, while our results show that the massive galaxy population is undergoing dramatic changes at this crucial epoch, they also suggest that the physical mechanisms which quench star formation activity are not simply connected to those responsible for the morphological transformation of massive galaxies into present-day giant ellipticals.

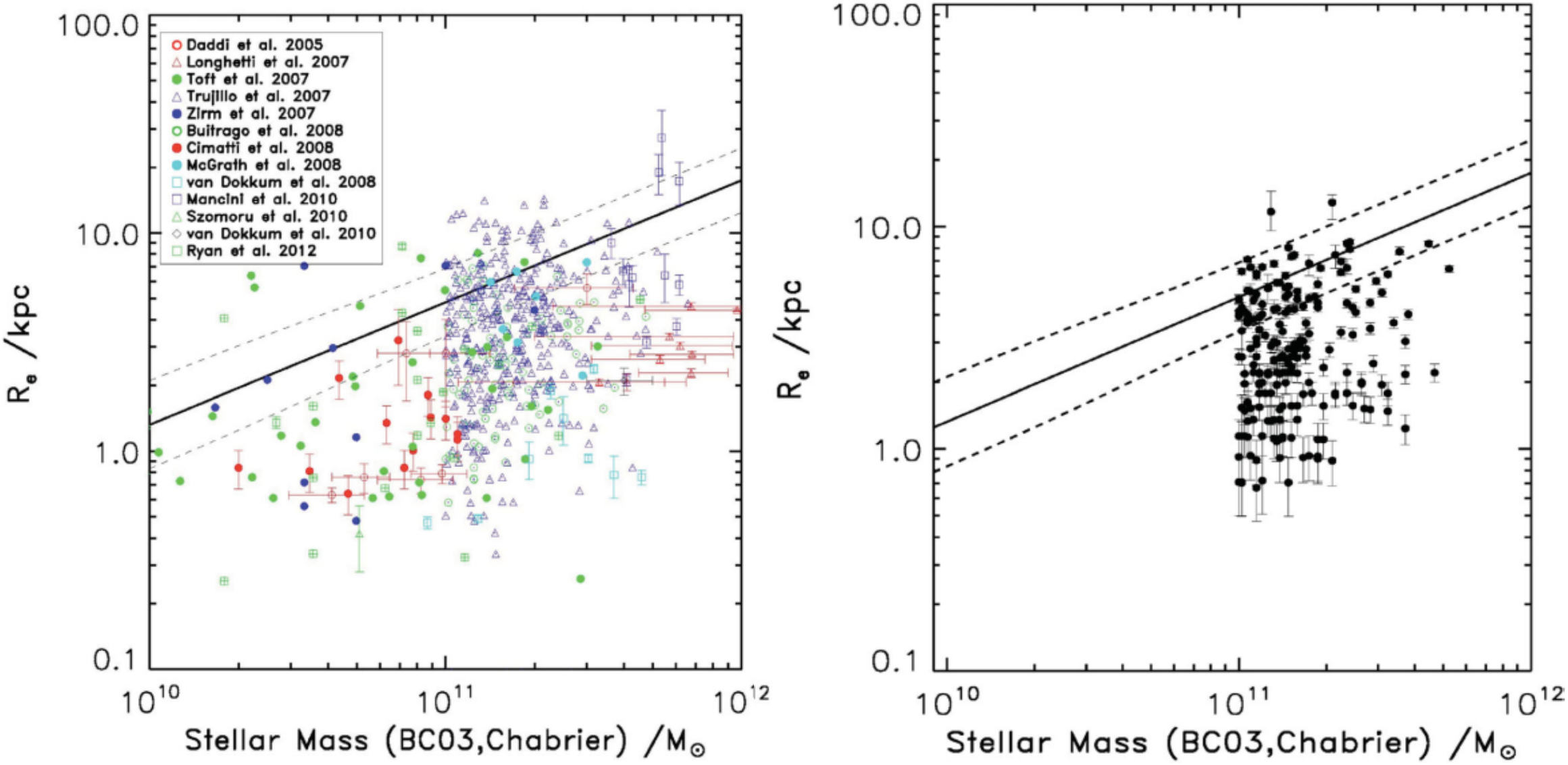

Figure 5. Various determinations of galaxy size versus stellar mass at $1 < z < 3$ from the literature are shown in the left-hand panel, for comparison with our new results for $M_* > 10^{11}\,M_\odot$ galaxies over the same redshift range as shown in the right-hand panel. In order to facilitate comparison of the semimajor axis scalelengths determined here with an appropriate low-redshift baseline we have plotted a solid line on both panels to indicate the local early-type galaxy relation from Shen et al. (2003) (with the scatter in this relation indicated by the dashed lines). Because the galaxy sizes determined by Shen et al. were determined by fitting 1D surface brightness profiles within circular apertures, we have converted their results to reflect estimated semimajor axis sizes by dividing the circularized Shen et al. sizes by the square root of the median axial ratio (b/a) for the $1 \times 10^{11} < M_* < 1 \times 10^{12}\,M_\odot$ SDSS sample. This median axial ratio value was taken to be 0.75, following the results from Holden et al. (2012). The results from the literature shown in the left-hand panel have all been converted to the masses that would have been derived using the Bruzual & Charlot (2003) models with a Chabrier IMF (see text for details). Unfortunately the scalelengths plotted in the left-hand panel contain a mix of both circularized and semimajor axis values, but since they come mainly from studies of early-type galaxies the correction from circularized back to semimajor axis values is generally small. Our own points shown in the right-hand panel are all based on Chabrier BC03 masses, and semimajor axis effective radii derived from our single-Sérsic modelling of the H_{160} images. This figure serves to demonstrate the extent to which our study has advanced knowledge of the size–mass relation for galaxies in this crucial redshift range in this high-mass regime. It can be seen that, while the majority of the objects in our sample lie below the local relation, a significant subset (32 ± 4 per cent) are consistent with it within the plotted 1σ errors.

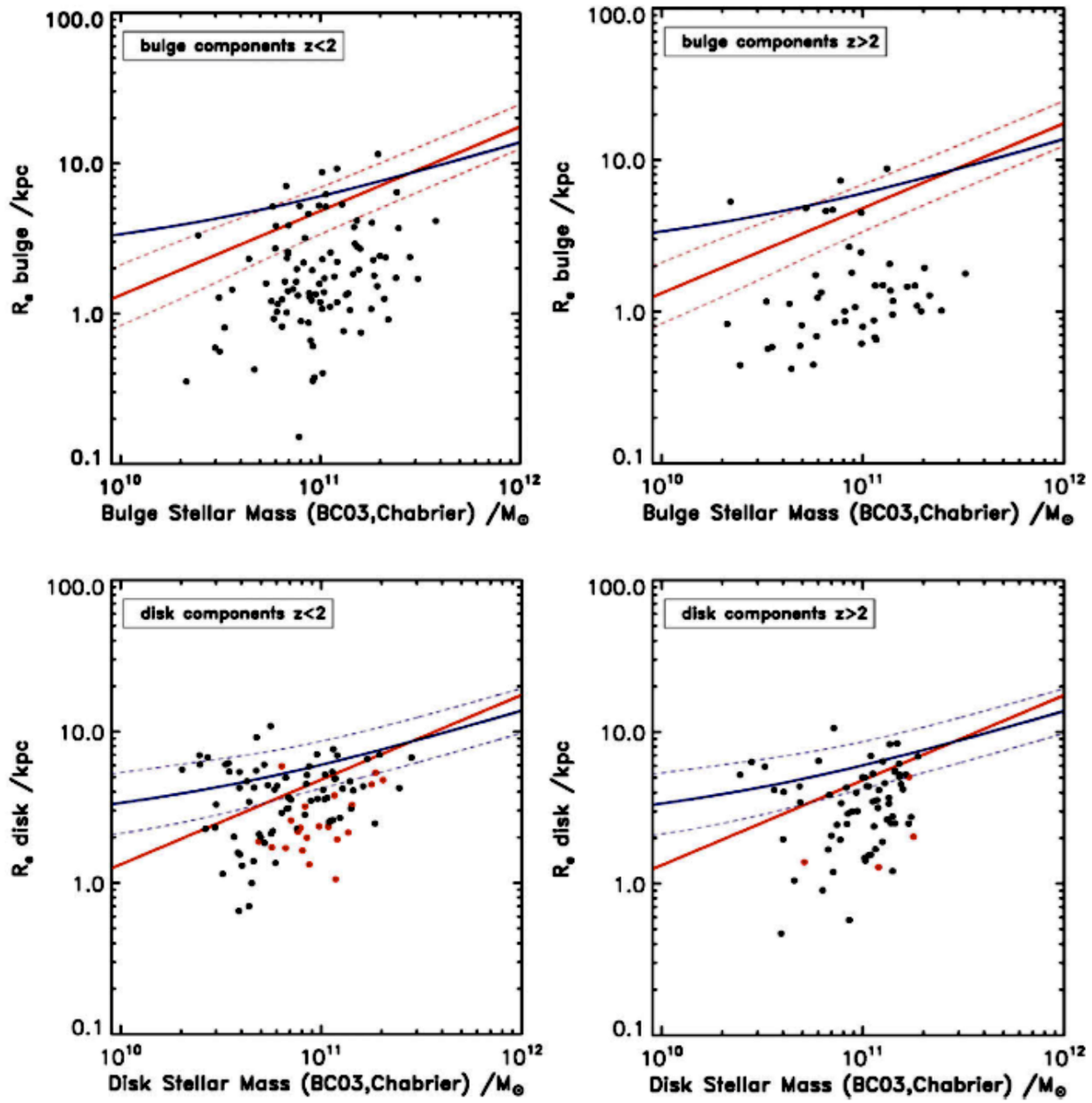

Figure 6. The size–mass relations displayed by the separate bulge components (upper row) and disc components (lower row) as produced from our bulge+disc modelling analysis of our massive galaxy sample (shown both for $1 < z < 3$ and then subdivided into two redshift bins). The masses plotted here for the individual subcomponents simply reflect the total mass of the 'parent' galaxy subdivided in proportion to the contribution of each component to the H_{160}-band light. For consistency, and to avoid overinterpreting the location of the weakest subcomponents, we have excluded nine objects whose component masses fall below $2 \times 10^{10}\,M_{\odot}$. In the lower row of plots, the disc components from the passive disc-dominated galaxies discussed in Section 6.3 (i.e. objects with sSFR $< 10^{-10}\,yr^{-1}$, no 24 μm counterparts and $B/T < 0/.5$) are overplotted in red. In order to provide a comparison with the sizes of comparably massive low-redshift bulge and disc counterparts, we have taken the local early-type and late-type galaxy relations from Shen et al. (2003) and converted them to non-circularized sizes [as described in the caption to Fig. 5, where the median axial ratio values were taken to be 0.75 for bulges (Holden et al. 2012) and 0.62 for discs (Padilla & Strauss 2008)]. These non-circularized relations are plotted as a solid red line for the local early-type relation, and a solid blue line for the local late-type galaxy relation; the dashed lines indicate the typical 1σ scatter in these relations. As discussed in detail in the text, these plots reveal the more dramatic size evolution displayed by the bulges which, by $z > 2$ are on average a factor of >4 smaller than their local counterparts. Nevertheless some bulges, and a rather large fraction of discs are still found to lie on the local relation throughout the redshift range.

Summary:

Complete, mass-selected sample of 200 galaxies with M∗ > 10^{11} Msun. virtually all the objects are destined to evolve into today's very massive $M∗ > 3\ 10^{11}$ Msun giant elliptical galaxies which display, at most, very low level disc components.

Considering the sample as a whole, our most basic statistical measurement is that

- the median size of these galaxies is 2.6 ± 0.2 kpc, a factor of 2.3 ± 0.1 smaller than the size of comparably massive galaxies today.
- the scatter in size is large, spanning 1 dex
- bulges display more rapid evolution to small sizes, both in terms of median size, and in terms of the relative numbers of objects which lie on and below the present-day size–mass relation.
- For the discs, 40 per cent lie on the local relation, with 60 per cent below, while for the bulges the percentage of objects which lie significantly below the local relation rises from an already high 80 per cent at $1 < z < 2$ to 85 per cent at $2 < z < 3$.
- Clearly bulges consistent with the local size–mass relation are rare at these redshifts and, moreover, the compact bulge population appears to become increasingly compact with increasing look-back time, lying a factor of 3.5 ± 0.5 below the local relation at $1 < z < 2$ but a factor of 4.4 ± 0.3 below at at $2 < z < 3$
- the objects which remain on the local relation, even out to the highest redshifts, are star-forming discs
- a clear trend for the massive galaxies become increasingly disc-dominated.

- Major mergers do not provide a sufficiently vertical evolutionary track on the size–mass plane to lift the compact high-redshift galaxies on to the present-day relation without yielding excessively high masses.

- In any case, size growth driven primarily by major mergers would require many more major mergers since z=2 than appears plausible from N-body simulations (which suggest <*2* per massive galaxy by the present day), or indeed from observed merger rates (e.g. Robaina et al. 2010).

- the bulk of the size growth must be attributed to minor mergers

    - which are much more effective at adding stars and dark matter in the outer regions of galaxies, increasing observed size with relatively limited increase in stellar mass.
    - minor mergers are more effective than major mergers at raising the dark matter to stellar mass ratio to the levels observed for the most massive galaxies today,
    - are better able to add mass while leaving the age and metallicity gradients in the central regions of massive galaxies unscrambled,
    - may provide a natural explanation for the kinematically decoupled cores frequently observed in present-day ellipticals

---

The presence of a significant population of passive discs among the massive galaxy population at these redshifts indicates that star formation activity can cease without a disc-galaxy being turned directly into a disc-free spheroid, as generally previously expected if the process that quenches star formation is a major merger.

Thus, while some fraction of the substantial population of star-forming discs may indeed suffer a major merger (possibly transforming rapidly into a compact passive spheroid, our results argue that another process must exist which is capable of terminating star formation activity while leaving a substantial disc intact.

A scenario which can account for star formation quenching, whilst still being consistent with the existence of passive discs, is the model of violent disc instabilities:

as the disc evolves, there is an inflow of mass to the centre of the disc, which gradually builds to form a massive bulge. This mass inflow can quench star formation whilst still retaining a massive disc in a process known as ‘morphology quenching’

Evolution of elliptical galaxies

Recent Structural Evolution of Early-Type Galaxies: Size Growth from z=1 to z=0
van der Wel etal 2008

Strong size and internal density evolution of early-type galaxies between z~2 and the present has been reported by several authors. Here we analyze samples of nearby and distant (z~1) galaxies with dynamically measured masses in order to confirm the previous, model-dependent results and constrain the uncertainties that may play a role. Velocity dispersion measurements are taken from the literature for 50 morphologically selected 0.8<z<1.2 field and cluster early-type galaxies with typical masses 2e11 Msol. Sizes are determined with ACS imaging. We compare the distant sample with a large sample of nearby (0.04<z<0.08) early-type galaxies extracted from the SDSS for which we determine sizes, masses, and densities in a consistent manner, using simulations to quantify systematic differences between the size measurements of nearby and distant galaxies. We find a highly significant structural difference between the nearby and distant samples, regardless of sample selection effects. The implied evolution in size at fixed mass between z=1 and the present is a factor of 1.97(0.15). This is in qualitative agreement with semianalytic models; however, the observed evolution is much faster than the predicted evolution. Our results reinforce and are quantitatively consistent with previous, photometric studies that found size evolution of up to a factor of 5 since z~2. A combination of structural evolution of individual galaxies through the accretion of companions and the continuous formation of early-type galaxies through increasingly gas-poor mergers is one plausible explanation of the observations.

From $\sigma_{\rm eff}$ and $R_{\rm eff}$ we derive the total dynamical mass and the corresponding average surface mass density within $R_{\rm eff}$:

$$M_{\rm dyn} = \frac{\beta R_{\rm eff} \sigma_{\rm eff}^2}{G}, \tag{2}$$

$$\Sigma_{\rm eff} = \frac{\beta \sigma_{\rm eff}^2}{2\pi G R_{\rm eff}}, \tag{3}$$

with $\beta = 5$, which has been shown to hold for local galaxies (Cappellari et al. 2006). Following Shen et al. (2003) we adopt the following characterization of the $M_{\rm dyn}$-$R_{\rm eff}$ relation:

$$R_{\rm eff} = R_c \left(\frac{M_{\rm dyn}}{M_c} \right)^b. \tag{4}$$

With a least-squares linear fit to all galaxies with mass $M_{\rm dyn} > 3 \times 10^{10}\ M_\odot$ we find that the slope is $b = 0.56$ and the zero point normalized to a characteristic mass $M_c = 2 \times 10^{11}\ M_\odot$ is $R_c = 4.80$ kpc. We find statistically

Theoretical expectations:

- A higher gas fraction in high-redshift galaxies leads to more dissipation and hence compact galaxies (e.g., Robertson et al. 2006; Khochfar & Silk 2006b)
- Subsequent evolution such as dry merging or accretion of smaller systems can increase the size of a galaxy (e.g., Loeb& Peebles 2003; Naab et al. 2007).

The models predict the strongest sample-averaged size evolution for the most massive galaxies (Khochfar & Silk 2006a) because of large differences in the gas fraction at different redshifts and because the assembly of massive galaxies continues until very late epochs in a hierarchical framework (e.g., De Lucia et al. 2006).

Observations:

- SDSS: Early-type galaxies with 0.04 < z< 0.08. The dispersion as measured within the spectroscopic aperture. Use GALFIT to determine effective radii from SDSS g-band imaging assuming R1/4-law
- Compilation of z=1-2 data: the Chandra Deep FieldYSouth (CDF-S) and the Hubble Deep FieldYNorth (HDF-N). In addition, we include galaxies in the massive, X-ray- selected cluster MS 1054 -0321 at z =0.831

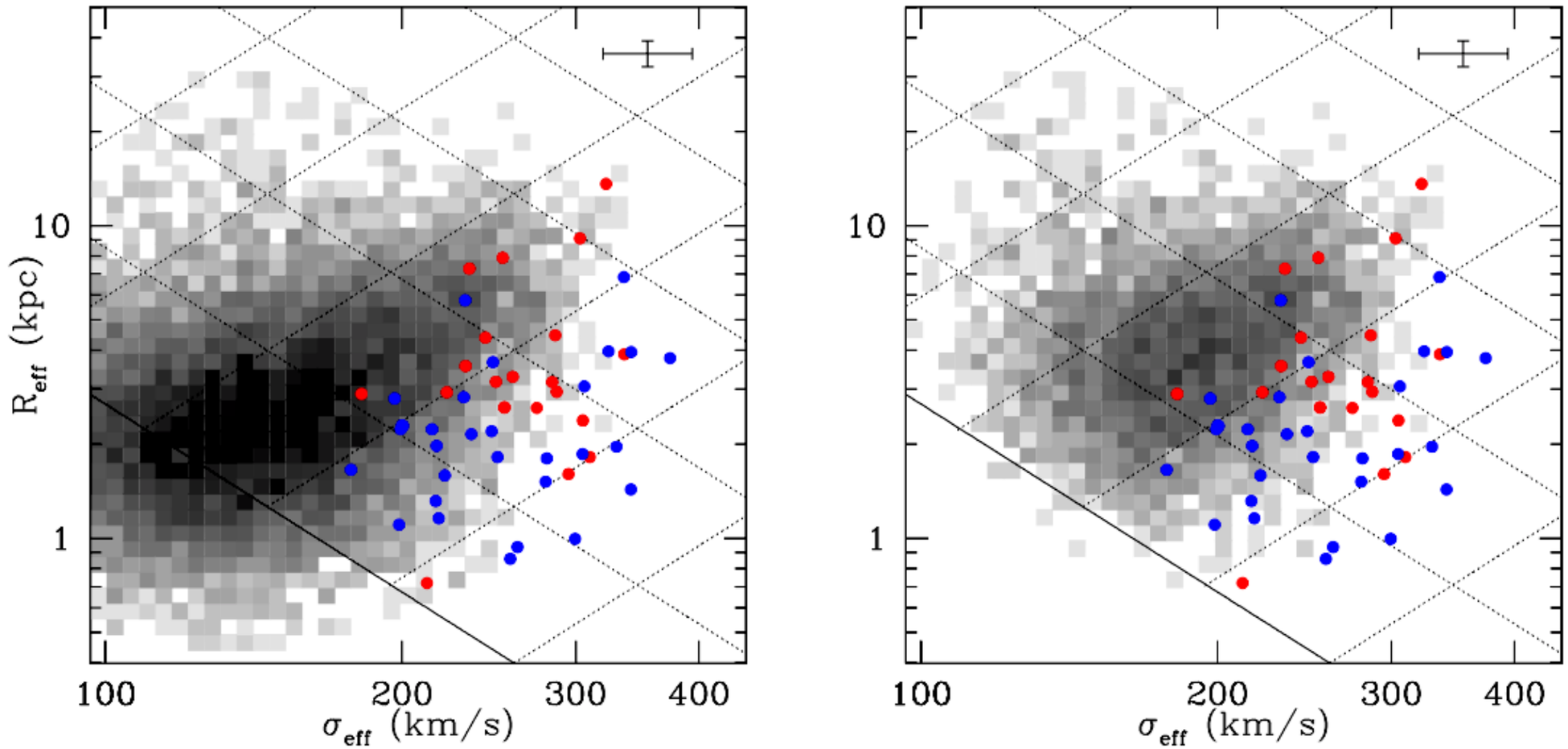

FIG. 3.— The $\sigma_{\rm eff}$-$R_{\rm eff}$ distributions of the nearby sample of early-type galaxies (*gray scale*) and the distant sample (data points). The red data points are cluster galaxies, and the blue data points are field galaxies. The error bars at the top right indicate the typical values of the errors for the distant sample. The solid line indicates $\log(M_{\rm dyn}) = 10.5$. Dotted lines indicate lines of constant $M_{\rm dyn}$ (*parallel to the solid line*), spaced by 0.5 dex, and lines of constant surface density $\Sigma_{\rm eff}$ (*perpendicular to the solid line*), also spaced by 0.5 dex. The left-hand panel shows the entire nearby sample; the right-hand panel only shows those galaxies in the nearby sample that would be included in the distant sample considering the selection effects, that apply to the surveys (see § 5.1). The highly significant offset (> 99.9% significance) between the local and distant samples implies significant structural evolution in the early-type galaxy population between $z \sim 1$ and the present.

Despite the large scatter, it is clear that the distant galaxies are offset from the nearby galaxies. Galaxies with the properties of typical galaxies in the distant sample ($\sigma_{\rm eff} \sim 250$ km s^{-1} ; $R_{\rm eff} \sim 3$ kpc) are rare in the local universe. In the nearby sample, galaxies with $\sigma_{\rm eff} \sim 250$ km s^{-1} have much larger sizes, and galaxies with sizes $R_{\rm eff} \sim 3$ kpc have dispersions of $\sigma_{\rm eff} \sim 150$ km s^{-1} . These numbers are only intended to guide the eye. A quantitative analysis of the differences between nearby and distant galaxies is presented below.

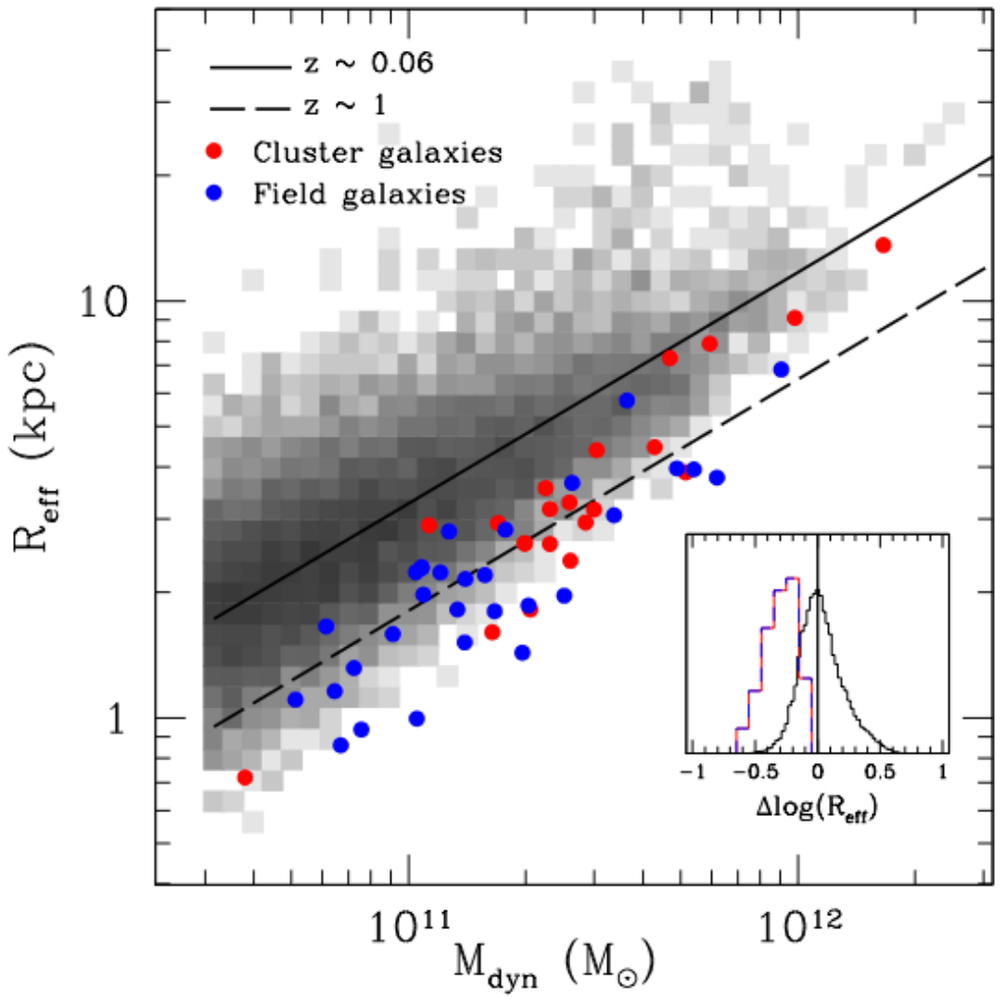

FIG. 4.— Mass-size relation for the nearby sample (*solid line*) and at $z \sim 1$ (*dashed line*); the symbols are the same as in Fig. 3. For the derivation of the $M_{\rm dyn}$-$R_{\rm eff}$ relation for the nearby sample see § 2.2; for the derivation of the $M_{\rm dyn}$-$R_{\rm eff}$ relation for the distant sample see § 5.2. The smaller, inset panel shows the distribution of the two samples around the $M_{\rm dyn}$-$R_{\rm eff}$ relation of the nearby sample (*the solid line in the large panel*). The distant galaxies are 1.8 ± 0.1 times smaller than the nearby galaxies. It appears that the most massive galaxies do not show as large an offset. This indicates that size evolution may be slower for the highest mass galaxies than for low-mass galaxies, but it has to be kept in mind that these very massive galaxies are brightest cluster galaxies and may therefore have developed differently from other galaxies.

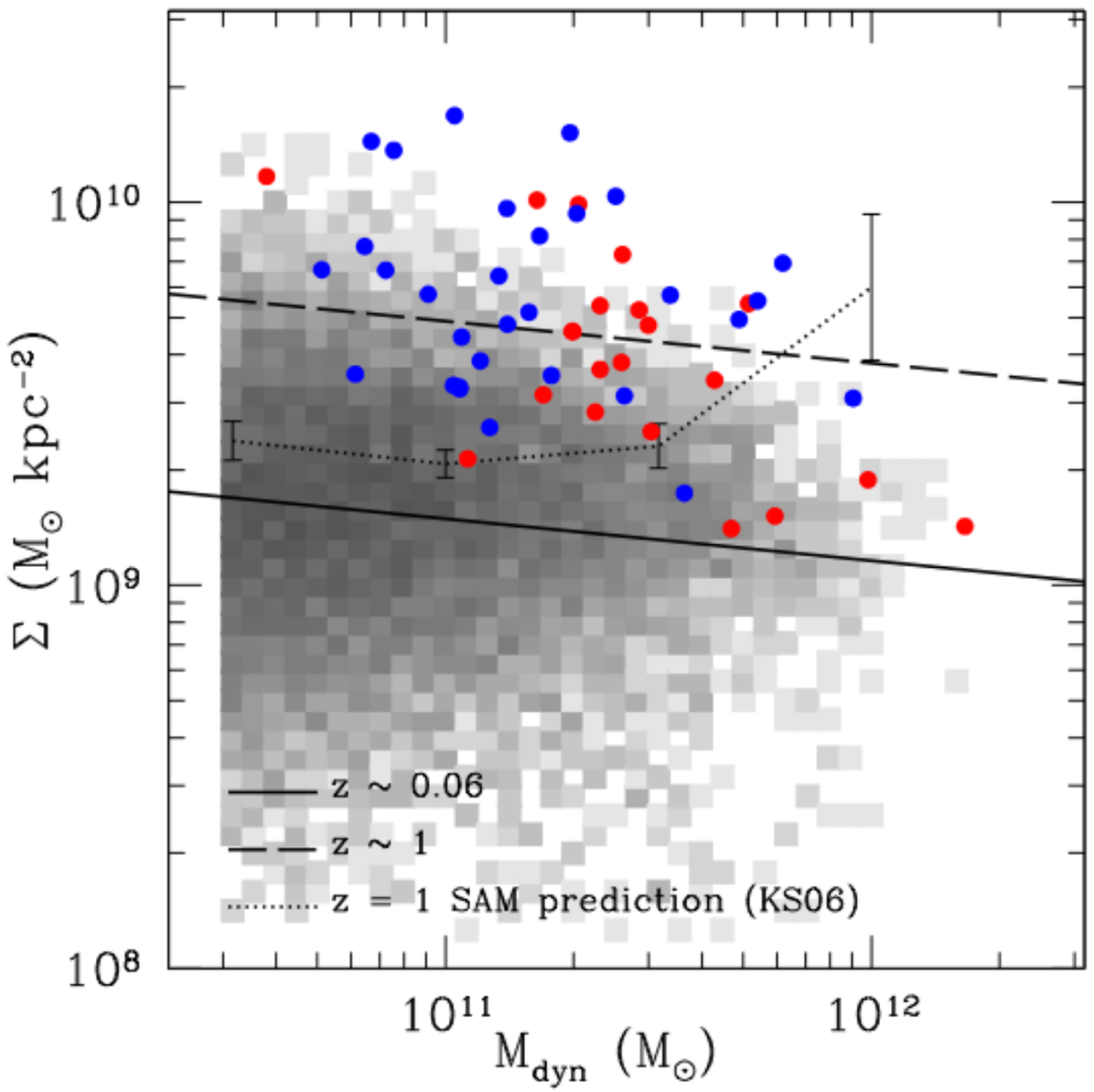

FIG. 5.— Mass-density relation at $z \sim 1$. The symbols and lines are the same as in Figs. 3 and 4. The $z \sim 1$ early-type galaxies are ~ 4 times more dense than their nearby counterparts. The prediction of the semianalytic size-evolution model for elliptical galaxies from Khochfar & Silk (2006a) is shown as the dotted line. The error bars indicate the predicted size evolution between $z = 0.8$ and $z = 1.2$, the redshift range of our distant sample. Despite qualitative agreement, there are significant quantitative differences between the predicted and observed evolution.

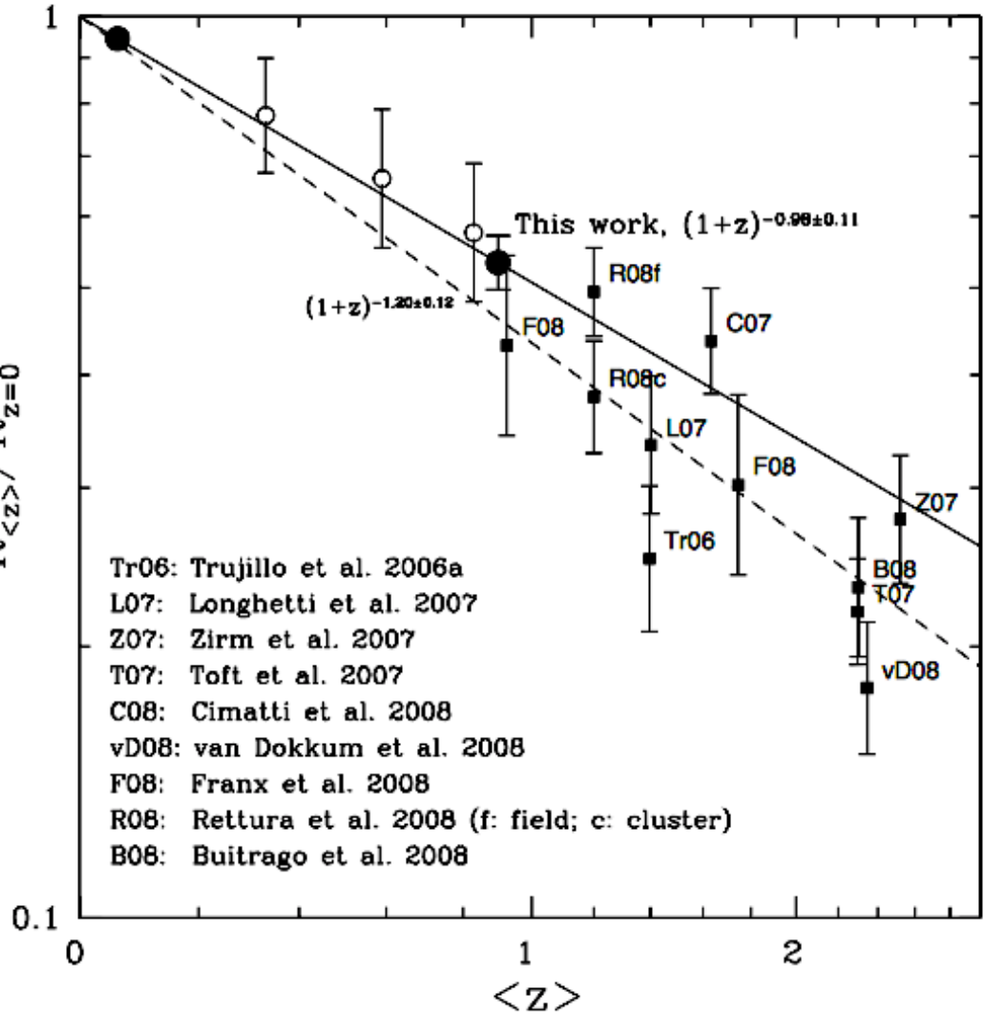

FIG. 6.— Size evolution with redshift as derived in this paper with dynamically determined masses (*large filled circles*) compared with previous results based on photometric masses (*small filled circles*). The solid line connects our samples at $z \sim 0.06$ and $z \sim 1$, the dashed line is a linear least-squares fit to the small filled data points. The open circles are samples of cluster galaxies with photometrically measured masses and serve as an illustration that size evolution shows a continuous trend between $z = 2.5$ and the present. The broad agreement in size evolution as derived from galaxies with dynamically and photometrically determines masses reinforces the conclusions of previous, photometric studies whose results were potentially mitigated by considerable systematic effects that do not affect our analysis.

ual galaxies. Numerical simulations have demonstrated that when early-type galaxies accrete neighbors without significant dissipational processes $\sigma_{\rm eff}$ does not change by much and that, to first order, $R_{\rm eff}$ increases linearly with mass. This does not depend strongly on the mass of the accreted object, i.e., the mass ratio of the merger (Boylan-Kolchin et al. 2005; Robertson et al. 2006; Boylan-Kolchin et al. 2006).

Simulations in a cosmological context show that an increase in size by a factor of 2 between $z \sim 1$ and the present is certainly possible (Naab et al. 2007). The strong observed size evolution thus argues in favor of a scenario in which significant mass from low-mass companions is accreted onto existing early-type galaxies over the past ∼7 Gyr, which also explains the broad tidal features that are frequently observed around early-type galaxies (van Dokkum 2005). As shown by Feldmann et al. (2008) such features are not necessarily, and are even quite unlikely to be, the result of major merger events and are most likely due to the accretion of low-mass, gas-poor satellites.